

Numerical implementation of the multiscale and averaging methods for quasi periodic systems

Tal Kachman

Department of Physics, Physics of Living Systems Group, Massachusetts Institute of Technology, Floor 6, 400 Tech Square, Cambridge, MA 02139,

Physics Department, Technion- Israel Institute of Technology, Haifa 3200, Israel

Shmuel Fishman

Physics Department, Technion- Israel Institute of Technology, Haifa 3200, Israel

Avy Soffer

Mathematics Department, Rutgers University, New-Brunswick, NJ 08903, USA

Abstract

We consider the problem of numerically solving the Schrödinger equation with a potential that is quasi periodic in space and time. We introduce a numerical scheme based on a newly developed multi-time scale and averaging technique. We demonstrate that with this novel method we can solve efficiently and with rigorous control of the error such an equation for long times. A comparison with the standard split-step method shows substantial improvement in computation times, besides the controlled errors. We apply this method for a free particle driven by quasi-periodic potential with many frequencies. The new method makes it possible to evolve the Schrödinger equation for times much longer than was possible so far and to conclude that there are regimes where the energy growth stops in-spite of the driving.

Keywords: Numerical solution, Time dependent potentials, Multiscale averaging

Email address: kachman@mit.edu (Tal Kachman)

1. Introduction

A method for the study of the dynamics for the Schrödinger equation with time dependent potentials [1] is implemented numerically. The potential is quasiperiodic in both space and time. The power of this new method is demonstrated. Exploration of the dynamics for such potentials is motivated by experiments in optics [2] where hypertransport, namely transport faster than ballistic was found experimentally and numerically in some regimes. In theoretical work that followed [2, 3, 4, 5] a classical theory was developed for the potentials relevant for these optics experiments. In particular, it was found in the framework of classical mechanics, that for smooth potentials the spreading in momentum as function of time stops. The calculations of the present paper are for such potentials. For short times, relevant for the existing experiments it was found that wave or quantum and classical dynamics agree in general features.

For long times it turned out impossible to compute numerically the quantum dynamics using the standard methods [6, 7], while with the method introduced in [1] and implemented here, calculations for such long times are feasible as will be demonstrated in this paper. Such calculations and comparison with the classical results, is of fundamental importance for the issue of quantum classical correspondence. The main objective of the present paper is to demonstrate the power of the method introduced in [1] for a physically relevant example.

Potentials which are quasiperiodic both in space and time, can manifest a high degree of complexity and are subject of many studies over the last decade, mostly in the framework of classical physics [8, 9, 10, 11, 12, 13, 14]. With different experimental realizations of such potentials there is also a need for a numerical approach to investigate them and their asymptotic behavior. The standard way to numerically solve time dependent potentials is based on either spectral methods [15, 16] or explicit/implicit finite difference schemes [7, 17]. In this paper we implement numerically a recently developed rigorously controlled multi-time scale averaging technique[1]. The above mentioned method has two distinct advantages. The first is that at each step of the averaging hierarchy

there is a well defined and completely known bound on the numerical error. The second advantage and one which has far greater impact is the reduction in computational time accompanied with each of the hierarchical averaging steps. This reduction enables us to go to long time scales, impossible by the methods we are aware of. In this paper we describe and present an implementation for a specific problem.

The outline of the paper is as follows. In Section 2, we present the model for which the method of multiple scale and averaging (MSA) is implemented. This model is of physical interest and importance. The MSA method that was developed in Ref. [1] and details of its implementation are presented in Secs. 3 and 4. For the convenience of readers the MSA method is summarized in the Appendix. The MSA method involves a hierarchy of computations where the first level is described in Sec. 3 and the following levels are presented in Section 4. The needed level is determined by the required precision and the time over which the system is evolved. In Section 5 we demonstrate that the MSA method is superior compared to the standard split step method, since for the same precision it is much faster. Moreover for the split step method there is only an empirical estimate on the error while for the MSA there is a rigorous bound. Using it in Section 6, we show that with the help of this method we could solve the Schrödinger equation for the model problem presented in Section 2, for an extremely long time; we conclude that for this model the energy does not grow to infinity in spite of the time dependent driving potential. The spreading in the quantum case is wider than in the corresponding classical system. This results from the fact that initially we observe a lot of spreading in the quantum case, while the classical case does not show spreading.

2. The model that will be studied

In this section we introduce the model for which our MSA method developed in [1] is implemented is introduced. In the first subsection its relation to physical systems is explained, while in the second section it is reduced to a form for which

the MSA method can be applied(see Eqs. 11-13).

2.1. The physical model

The random potentials which are prepared in optics [18, 2] and atom optics [19, 20, 21] experiments, are described by a sum of random Fourier components. In experiments, potentials which are composed out of a large number of random independent Fourier components N , are created .

More specifically here, the Schrödinger equation for a potential

$$V(x', \tau) = \frac{1}{\sqrt{N}} \sum_{n=1}^N A_n \exp(i(k_n x' - \omega'_n \tau)) + \mathcal{C.C} \quad (1)$$

is used. The A_m are independent, identically distributed complex random variables, $\mathcal{C.C}$ stands for complex conjugate. The expectation values of these variables satisfy

$$\langle A_m \rangle = \langle A_m A_n \rangle = 0 \quad \langle A_m A_n^* \rangle = \sigma^2 \delta_{nm} \quad (2)$$

We will study the specific model where $A_n = A e^{i\phi_m}$ with ϕ_m uniformly distributed in the interval $[-\pi, \pi]$ and $A > 0$. The distribution of ω_n and k_n is specified in Section 5.

The equation of motion is the time dependent Schrödinger equation

$$i\partial_\tau \psi(x', \tau) = H\psi(x', \tau). \quad (3)$$

Where

$$H = \frac{1}{2}p'^2 + V(x', \tau), \quad (4)$$

$$p' = -i\nabla_{x'}.$$

In the following section we will introduce the reduction of the problem to a form where the MSA technique is applicable.

2.2. Reduction of the problem

In the model with potential given by (1), the particle is expected to be accelerated most effectively in the regime of velocities where the Chirikov resonances

$$v_n^{(\tau)} = \frac{\omega'_n}{k_n} \quad (5)$$

are formed [22, 23].

In this paper we choose $v_n^{(r)}$ and k_n uniformly distributed in the intervals $[v^{(\min)}, v^{(\max)}]$ and $[k^{(\min)}, k^{(\max)}]$ respectively. The crucial point is that the Chirikov resonant velocities are bounded in a phase space strip. This is typically the case for smooth potentials, and will be assumed in this paper.

Here we would like to study what is the acceleration of a particle prepared with momentum or velocity v (we assume unit mass), so that all $v_n^{(r)}$ are far from v . For the classical corresponding system we found that the acceleration is negligible[3, 5, 4]. Here we study the corresponding quantum mechanical system. For this purpose it is convenient to work in a frame of reference where the initial velocity of the particle vanishes. For this we perform the Galilean transformation

$$x = x' - v\tau, \quad (6)$$

where v is the velocity of the moving frame (in later stages we will relate this quantity to the required small parameter) on the potential (1)

$$\begin{aligned} V(x + v\tau, \tau) &= \frac{A}{\sqrt{N}} \sum_{n=1}^N \cos(k_n(x + v\tau) - \omega'_n\tau + \phi_n) \\ &= \frac{A}{\sqrt{N}} \sum_{n=1}^N \cos(k_n x + (k_n v - \omega'_n)\tau + \phi_n). \end{aligned} \quad (7)$$

Now, re-scaling time as

$$t = \tau v, \quad (8)$$

the potential takes the form

$$V(x, t) = \frac{A}{\sqrt{N}} \sum_{n=1}^N \cos\left(k_n x - \frac{(\omega'_n - k_n v)}{v} t + \phi_n\right) \quad (9)$$

and defining

$$\omega_n = \frac{(\omega'_n - k_n v)}{v} \quad (10)$$

The potential in the moving frame takes the form

$$V(x, t) = \frac{A}{\sqrt{N}} \sum_{n=1}^N \cos(k_n x - \omega_n t + \phi_n) \quad (11)$$

The time dependent Schrödinger equation is

$$i\partial_t\psi(x,t) = \frac{1}{v}H(p,x,t)\psi(x,t) \quad (12)$$

Introducing the small parameter $\beta = \frac{1}{v}$:

$$i\partial_t\psi(x,t) = \beta H(p,x,t)\psi(x,t) \quad (13)$$

From this point on we will use the small parameter β to perform the averaging steps introduced in the next section. In what follows we will also relate the small parameter β to time scale on which we average. The Hamiltonian will be approximated by a finite matrix (in space and momentum) and it will be verified that the spreading never reaches the boundaries set by this basis.

3. The averaging scheme

The multiscale averaging method is based on replacing the original Hamiltonian by a hierarchical set of averaged Hamiltonians. In each step we perform a “peel-off” transformation and average a part of the Hamiltonian, for a chosen time interval of length $T_0 = \frac{1}{\sqrt{\beta}} = \sqrt{v}$. This choice is not unique, but as shown in [1] leads to effective error bounds. We use the fact that Eq (13) is of the form of (2.1) in [1].

In this section the implementation of the MSA method of [1] for equation (13) will be presented. In Appendix A we summarize the main results of Ref. [1]

3.1. Zero order

The zero order average on the j th time interval has the form ($V(t) \equiv V(x,t)$)

$$\bar{V}_0^{(j)} = \frac{1}{T_0} \int_{jT_0}^{(j+1)T_0} V(t) dt \quad (14)$$

In the case of the potential (1), the zero order averaging can be performed analytically

$$\begin{aligned}
\bar{V}_0^{(j)} &= \frac{1}{T_0} \int_{jT_0}^{(j+1)T_0} V(t) dt = \frac{A}{\sqrt{N}T_0} \int_{jT_0}^{(j+1)T_0} \sum_{n=1}^N \cos(k_n x - \omega_n t + \phi_n) = \\
&= \frac{A}{\sqrt{N}T_0} \sum_{n=1}^N \frac{1}{\omega} [\sin(k_n x - \omega_n (j+1)T_0 + \phi_n) \\
&\quad - \sin(k_n x - \omega_n jT_0 + \phi_n)] = \\
&= 2 \frac{A}{\sqrt{N}T_0} \sum_{n=1}^N \frac{1}{\omega_n} \sin\left(\frac{1}{2}\omega_n T_0\right) \cos\left(k_n x - \omega_n \left(j + \frac{1}{2}\right)T_0 + \phi_n\right) \quad (15)
\end{aligned}$$

This defines the Hamiltonian on one time interval; accordingly we can write the Hamiltonian of one interval as

$$\bar{H}_0^{(j)}(x) = -\frac{1}{2} \frac{\partial^2}{\partial x^2} + \bar{V}_0^{(j)}(x) \quad (16)$$

The global Hamiltonian corresponding to (2.1) of [1] (see appendix), which gives the zeroth order approximation to $H(t)$, is generated by:

$$\bar{H}_0^g = \bar{H}_0^{(j)}(t) \quad \text{for } jT_0 \leq t < (j+1)T_0. \quad (17)$$

Using this notation, a general time evolution can be written as the product of the interval propagators since \bar{H}_0^g is piecewise constant in time.

$$U_0(t) = e^{-i\beta \bar{H}_0^{(j_{max})}(t-j_{max}T_0)} \dots e^{-i\beta \bar{H}_0^{(1)}T_0} e^{-i\beta \bar{H}_0^{(0)}T_0} \quad (18)$$

where $j_{max} - 1$ is the integer part of t/T_0 . The evolution in this order is

$$\psi_0(x, t) = U_0(t) \psi(x, 0). \quad (19)$$

The propagator satisfies

$$i \frac{\partial}{\partial t} U_0(t) = \beta \bar{H}_0^{(g)} U_0(t) \quad (20)$$

corresponding to (2.10) of [1]. This propagator is numerically implemented and used to solve the time dependent equation of motion. The error in this order is bounded by $\beta^{\frac{1}{2}}$ up to times of order T_0 , the reasoning behind this is shown in the appendix.

3.2. First order

The first order averaging is based upon a “peel-off” transformation of the zero order. In such a transformation the next order Hamiltonian is constructed from the zero order in the following way: Let $H_1(t)$ be defined as

$$H_1(t) = U_0^{-1}(t) [H(t) - \bar{H}_0^g(t)] U_0(t) \quad (21)$$

and its average in the j -th interval is

$$\bar{H}_1^{(j)} = \frac{1}{T_0} \int_{jT_0}^{(j+1)T_0} H_1(t) dt \quad (22)$$

we have that $H(t) = [H_1(t) - \bar{H}_0^g] + \bar{H}_0^g$. Hence $H_1(t)$ is the Heisenberg dynamics of the full problem with $U_0(t)$ dynamics peeled off. An important point to note is that the Laplacian term drops in H_1 ! Hence $H_1(t)$ is a bounded operator, for which the results of [1] directly apply. The $\bar{H}_1(t)$ propagator is

$$U_1(t) = e^{-i\beta \bar{H}_1^{(j_{max})}(t-j_{max}T_0)} \dots e^{-i\beta \bar{H}_1^{(0)}T_0} \quad (23)$$

so, the $\psi_1(t)$ dynamics is

$$\psi_1(t) = U_0(t) U_1(t) \psi(0).$$

Before diagonalizing this operator in order to calculate the time evolution, there are several steps needed to be taken. First we write explicitly $\bar{H}_1^{(j)}$ using integration by parts

$$\bar{H}_1^{(j)} = \frac{1}{T_0} \int_{jT_0}^{(j+1)T_0} U_0^{-1}(t) [H(t) - \bar{H}_0^g(t)] U_0(t) dt = \bar{H}_1^{(j,I)} + \bar{H}_1^{(j,II)} + \bar{H}_1^{(j,III)}, \quad (24)$$

where

$$\bar{H}_1^{(j,I)} = \frac{1}{T_0} \left[U_0^{-1}(t) \left(\int_0^t [H(t') - \bar{H}_0^g(t')] dt' \right) U_0(t) \right]_{t=jT_0}^{(j+1)T_0} \quad (25)$$

$$\bar{H}_1^{(j,II)} = -\frac{1}{T_0} \int_{nT_0}^{(n+1)T_0} dt' \left(\frac{\partial}{\partial t'} U_0^{-1}(t') \right) \left[\int_0^{t'} [H(s) - \bar{H}_0^g(s)] ds \right] U_0(t'), \quad (26)$$

and

$$\bar{H}_1^{(j,\text{III})} = -\frac{1}{T_0} \int_{jT_0}^{(j+1)T_0} U_0^{-1}(t') \left[\int_0^{t'} [H(s) - \bar{H}_0^g(s)] ds \right] \left(\frac{\partial}{\partial t} U_0 \right) (t') dt'. \quad (27)$$

We note that for any integer t/T_0 ,

$$\int_{jT_0}^{(j+1)T_0} [H(t') - \bar{H}_0^g(t')] dt' = 0 \quad (28)$$

by construction. Therefore $\bar{H}_1^{(j,\text{I})}(t) = 0$ and $\bar{H}_1^{(j,\text{II})}(t)$ can be simplified.

Moreover the expression in $\bar{H}_1^{(j,\text{III})}$ is just the hermitian conjugate of $\bar{H}_1^{(j,\text{II})}$

so we only need to analyze the second term:

$$\begin{aligned} \bar{H}_1^{(j,\text{II})} &= \frac{1}{T_0} \int_{jT_0}^{(j+1)T_0} dt' \left(\frac{\partial}{\partial t'} U_0^{-1}(t') \right) \left[\int_{jT_0}^{t'} [H_j(s) - \bar{H}_0^{(j)}(s)] ds \right] U_0(t') \quad (29) \\ &= \frac{1}{T_0} \int_{jT_0}^{(j+1)T_0} dt' \left(\frac{\partial}{\partial t'} U_0^{-1}(t') \right) \left[\int_{jT_0}^{t'} H_0(s) ds - (t' - jT_0) \bar{H}_0^{(j)} \right] U_0(t') \end{aligned}$$

To evaluate this operator we can use a recursive construction of states based on the zeroth order eigenstates of the averaged Hamiltonian. It is important to remember that this is actually a matrix. For convenience of notation we will define

$$U_0(t) = e^{-i\beta \bar{H}_0^{(j)}(t-jT_0)} \dots e^{-i\beta \bar{H}_0^{(1)}T_0} e^{-i\beta \bar{H}_0^{(0)}T_0}, \quad (30)$$

For t that is an integer multiple of T_0 that will be assumed in all of our calculations

$$U_0(t) = \prod_{j'=0}^j W_{j-j'} \quad (31)$$

where

$$W_j(t) = e^{-i\beta \bar{H}_0^{(j)}T_0}. \quad (32)$$

The eigenvalues and eigenfunctions of $\bar{H}_0^{(j)}$ are

$$\bar{H}_0^{(j)} |\varphi_j^k\rangle = E_j^k |\varphi_j^k\rangle \quad (33)$$

For a base of size M (that is assumed to be finite and we take $M = 64$) the eigenfunctions are approximately eigenfunctions of a free particle, namely

$$\langle x | \varphi_j^k \rangle \approx e^{ikx}. \quad (34)$$

We will have M eigenvalues and eigenvectors, the largest value of $|\tilde{k}|$ is 50. Between each pair of propagators W_j, W_{i+1} we can insert the identity resolution in the corresponding basis (33)

$$\hat{I}_j = \sum_{k=1}^M |\varphi_j^k\rangle \langle \varphi_j^k| \quad (35)$$

resulting in

$$U_0(t) = W_j \cdots W_1 W_0 = W_j \hat{I}_j \cdots W_1 I_1 W_0 I_0 \quad (36)$$

As an example let us take just the first two terms

$$W_1 I_1 W_0 I_0 = \sum_{k_1=1}^M W_1 |\varphi_1^{k_1}\rangle \langle \varphi_1^{k_1}| \sum_{k_0=1}^M W_0 |\varphi_0^{k_0}\rangle \langle \varphi_0^{k_0}| \quad (37)$$

the brackets expressions are just scalars, and since our potential is diagonal this reduces to the sum of eigenvalues $E_j^{k_j}$

$$\begin{aligned} W_1 I_1 W_0 I_0 &= \sum_{k_1=1}^M W_1 |\varphi_1^{k_1}\rangle \langle \varphi_1^{k_1}| W_0 \sum_{k_0=1}^M |\varphi_0^{k_0}\rangle \langle \varphi_0^{k_0}| \\ &= \sum_{k_1=1}^M e^{-i\beta T_0 E_1^{k_1}} |\varphi_1^{k_1}\rangle \langle \varphi_1^{k_1}| \sum_{k_0=1}^M e^{-i\beta T_0 E_0^{k_0}} |\varphi_0^{k_0}\rangle \langle \varphi_0^{k_0}| \end{aligned} \quad (38)$$

using the notation

$$\alpha_{k_1 k_0} = \langle \varphi_1^{k_1} | \varphi_0^{k_0} \rangle \quad (39)$$

this becomes

$$W_1 I_1 W_0 I_0 = \sum_{k_0=1}^M \sum_{k_1=1}^M \alpha_{k_1 k_0} e^{-i\beta T_0 E_1^{k_1}} e^{-i\beta T_0 E_0^{k_0}} |\varphi_1^{k_1}\rangle \langle \varphi_1^{k_1}| \quad (40)$$

In the same way for the complete sequence of propagators

$$\begin{aligned} U_0(t) = \prod_{j'=0}^j W_{j-j'} &= \prod_{j'=0}^j [W_{j-j'} I_{j-j'}] = \sum_{k'_0=1}^M \cdots \sum_{k'_j=1}^M \sum_{k_0=1}^M \cdots \sum_{k_j=1}^M \alpha_{k_j k_{j-1}} \alpha_{k_{j-1} k_{j-2}} \cdots \\ &\quad \cdots \alpha_{k_1 k_0} e^{-i\beta(t-jT_0) E_j^{k_j}} \cdots e^{-i\beta T_0 E_1^{k_1}} e^{-i\beta T_0 E_0^{k_0}} |\varphi_j^{k_j}\rangle \langle \varphi_0^{k_0}| \end{aligned} \quad (41)$$

and

$$i \frac{\partial}{\partial t} U_0(t) = \beta \bar{H}_0^{(g)}(t) U_0(t). \quad (42)$$

The inverse takes the form

$$\begin{aligned} U_0^{-1}(t) &= e^{i\beta \bar{H}_0^{(0)} T_0} e^{i\beta \bar{H}_0^{(1)} T_0} \dots e^{i\beta \bar{H}_0(t-jT_0)} = \prod_{j'=0}^j W_{j'}^\dagger \\ &= \sum_{k_j=1}^M \dots \sum_{k_{j-1}=1}^M \alpha_{k_0 k_1}^* \alpha_{k_1 k_2}^* \dots e^{i\beta(t-jT_0)E_0} e^{i\beta(j-1)E_0} |\varphi_0^{k_0}\rangle \langle \varphi_j^{k_j}| \end{aligned} \quad (43)$$

and

$$\frac{\partial}{\partial t} U_0(t) = - \sum_{k'_0=1}^M \dots \sum_{k'_j=1}^M \sum_{k_0=1}^M \dots \sum_{k_j=1}^M i\beta E_j^{k_j} \alpha_{k_j k_{j-1}} \alpha_{k_{j-1} k_{j-2}} \dots \alpha_{k_1 k_0} P(j) \quad (44)$$

$$P(j) = e^{-i\beta(t-jT_0)E_j^{k_j}} \dots e^{-i\beta T_0 E_0^{k_0}} |\varphi_j^{k_j}\rangle \langle \varphi_0^{k_0}|$$

$$\frac{\partial}{\partial t} U_0^{-1}(t) = \sum_{k_j=1}^M \dots \sum_{k_{j-1}=1}^M \alpha_{k_0 k_1}^* \alpha_{k_1 k_2}^* \dots \alpha_{k_{j-1} k_j}^* e^{i\beta T_0 E_0^{k_0}} \dots e^{i\beta(t-jT_0)E_j^{k_j}} i\beta E_j^{k_j} |\varphi_0^{k_0}\rangle \langle \varphi_j^{k_j}| \quad (45)$$

The full form of $\bar{H}_1^{(j, \text{II})}$ is

$$\begin{aligned} \bar{H}_1^{(j, \text{II})}(t) &= -\frac{1}{T_0} \sum_{k'_0=1}^M \dots \sum_{k'_j=1}^M \sum_{k_0=1}^M \dots \sum_{k_j=1}^M \beta E_j^{k_j} \alpha_{k'_0 k'_1}^* \dots \alpha_{k'_{j-1} k'_j}^* \alpha_{k_j k_{j-1}} \dots \alpha_{k_1 k_0} \\ &\quad \int_{jT_0}^{(j+1)T_0} dt' e^{i\beta T_0 E_0^{k'_0}} e^{-i\beta T_0 E_0^{k'_0}} \dots e^{i\beta(t-jT_0)E_j^{k'_j}} e^{-i\beta(t'-jT_0)E_j^{k'_j}} \\ &\quad |\varphi_0^{k'_0}\rangle \langle \varphi_j^{k'_j}| \left[\int_{jT_0}^{t'} H(s) ds - (t' - jT_0) \bar{H}_0^{(j)} \right] |\varphi_j^{k_j}\rangle \langle \varphi_0^{k_0}| = \\ &= -\frac{1}{T_0} \sum_{k'_0=1}^M \dots \sum_{k'_j=1}^M \sum_{k_0=1}^M \dots \sum_{k_j=1}^M \beta E_j^{k_j} \alpha_{k'_0 k'_1}^* \dots \alpha_{k'_{j-1} k'_j}^* \alpha_{k_j k_{j-1}} \dots \alpha_{k_1 k_0} \\ &\quad \int_{jT_0}^{(j+1)T_0} dt' e^{-i\beta T_0 E_0^{k'_0}} \dots e^{i\beta(t-jT_0)E_j^{k'_j}} e^{-i\beta(t-jT_0)E_j^{k'_j}} \\ &\quad \left\langle \varphi_{k_j}^j \left| \int_{jT_0}^{t'} H(s) ds - (t - jT_0) \bar{H}_0^{(j)} \right| \varphi_j^{k'_j} \right\rangle |\varphi_0^{k'_0}\rangle \langle \varphi_0^{k_0}| \quad (46) \end{aligned}$$

Finally the full expression for the first order averaged Hamiltonian is

$$\bar{H}_1^{(j)}(t) = \bar{H}_1^{(j, \text{II})}(t) + \left(\bar{H}_1^{(j, \text{II})}(t) \right)^\dagger \quad (47)$$

$$\begin{aligned}
\bar{H}_1^{(j)}(t) &= 2\Re \left\{ -\frac{1}{T_0} \sum_{k'_0=1}^M \cdots \sum_{k'_j=1}^M \sum_{k_0=1}^M \cdots \sum_{k_j=1}^M \beta E_j^{k_j} \alpha_{k'_0 k'_1}^* \cdots \alpha_{k'_{j-1} k'_j}^* \right. & (48) \\
&\quad \alpha_{k_j k_{j-1}} \cdots \alpha_{k_1 k_0} \int_{jT_0}^{(j+1)T_0} e^{-i\beta T_0 E_0^{k'_0}} \cdots e^{i\beta(t-jT_0) E_j^{k'_j}} e^{-i\beta(t-jT_0) E_j^{k'_j}} \\
&\quad \left. dt' \left\langle \varphi_j^{k_j} \left| \int_{jT_0}^{t'} H(s) ds - (t-jT_0) \bar{H}_0^{(j)} \right| \varphi_j^{k'_j} \right\rangle \right\} |\varphi_0^{k'_0}\rangle \langle \varphi_0^{k_0}|
\end{aligned}$$

At first sight this expression might seem very complicated but can be understood quite easily; in fact what we have here is a matrix constructed from the sum of matrix products; the terms of the matrix involve only the products of the zero order eigenvalues and eigenvector (the eigenvalues and eigenvectors of the zeroth order averaged Hamiltonian). The benefit of calculating the propagator in this manner is that one only needs to diagonalize the Hamiltonian in each interval only once. The error in this order is β up to times T_0^3 , as is reasoned in the appendix.

3.3. Normal form transformation

To improve the accuracy we implement the normal form transformation; we will use the form given in Eq. (3.10) of [1]. In our notation this becomes

$$\tilde{U}_1(t) = 1 + i\beta U_1^{-1}(t) \left(\int_0^t [H_1(t') - \bar{H}_1^g(t')] dt' \right) U_1(t). \quad (49)$$

The manner in which we will simplify the above expression will be similar to the method used to calculate U_1 and H_1 given in Eq (23) and (20), splitting into intervals of length T_0 and using (28), replacing H by H_1 :

$$\begin{aligned}
\tilde{U}_1(t) &= 1 + i\beta U_1^{-1} \left(\sum_{j'=0}^j \int_{j'T_0}^{(j'+1)T_0} dt' [H_1(t') - \bar{H}_1^{(j')}] \right) & (50) \\
&\quad + \int_{jT_0}^t [H_1(t') + \bar{H}_1^{(j)}(t')] dt' U_1(t).
\end{aligned}$$

Therefore

$$\begin{aligned}
\tilde{U}_1(t) &= 1 + i\beta U_1^{-1} \int_{jT_0}^t [H_1(t') - \bar{H}_1^{(j)}(t')] dt' U_1(t) = & (51) \\
&\quad 1 + i\beta U_1^{-1} \left[\left(\int_{jT_0}^t H_1(t') dt' \right) - (t-jT_0) \bar{H}_1^{(j)} \right] U_1(t)
\end{aligned}$$

and explicitly

$$\begin{aligned}\tilde{U}_1(t) &= 1 + i\beta e^{i\beta\bar{H}_1^{(0)}T_0} \dots e^{i\beta\bar{H}_1^{(j)}(t-jT_0)} \left[\left(\int_{jT_0}^t H_1(t') dt' \right) - (t-jT_0)\bar{H}_1^{(j)} \right] U_1(t) \\ & \quad (52) \\ U_1(t) &= e^{-i\beta\bar{H}_1^{(j)}(t-jT_0)} \dots e^{-i\beta\bar{H}_1^{(0)}T_0}.\end{aligned}$$

For numerical convenience we defined

$$W_j^0(t) = e^{i\beta H_1^{(j)}(t-jT_0)} \left[\left(\int_{jT_0}^t H_1(t') dt \right) - (t-jT_0)\bar{H}_1^{(j)} \right] \quad (53)$$

where the product is performed using the resolution of the identity (35) and then performing $j-1$ times the transformation

$$\tilde{U}_1(t) = W_0^* \dots W_{j-1}^* W_j^* W_j W_{j-1} \dots W_0. \quad (54)$$

If also the normal form transformation is performed the error is $\beta^{\frac{3}{2}}$ up to times $T_0^{3/4}$ where W_j is given by (32). This relation can be computed recursively. The operation leading from $U(t)$ to $\tilde{U}_1(t)$ can be applied to $\tilde{U}_1(t)$ resulting in a hierarchy of operations of exponentially improving accuracy where in this section the first level was obtained and the next level will be described in the following Section.

4. Iterative application of error analysis

We turn now to estimate rigorously the errors using the multi-scale and averaging method.

Recall that the MSA method works by solving

$$i \frac{\partial U}{\partial t} = \beta A(t) U \quad (55)$$

with β small on a time interval of order $\beta^{\frac{1}{2}} \equiv T_0$. Let us denote by t_{max} the maximum time we want to simulate dynamics. After introducing a normal form transformation we eliminate the $c\beta^{\frac{1}{2}}$ error term [1], and we get

$$U(t) = U_0(t)R_0(t) \quad \text{for } 0 \leq t \leq t_{max} \quad (56)$$

with $R(t) = \mathcal{O}\left(\beta^{\frac{3}{2}} t_{max}\right)$ for $0 \leq t \leq t_{max}$ with $U_0(t)$ is given by (a product of) averaged dynamics followed by a normal form unitary transformation. Moreover

$$i \frac{\partial R_0}{\partial t} = \beta^{\frac{3}{2}} A_1(t) R_0(t), \quad (57)$$

with

$$\|A_1(t)\| = \mathcal{O}(1). \quad (58)$$

If we then use the same method of averaging on $R_0(t)$ Eq. (57) we get $R_0(t) = U_1(t)R_1(t)$ and

$$U(t) = \tilde{U}_0(t) U_1(t) R_1(t) \quad (59)$$

where now $U_1(t)$ is the averaged approximate solution for $R_0(t)$, and

$$R_1(t) = \mathcal{O}\left(\beta^{\frac{3}{2}}\right) + \mathcal{O}\left(\left(\beta^{\frac{3}{2}}\right)^{\frac{3}{2}} t_{max}\right). \quad (60)$$

Again after normal form transformation, the $\mathcal{O}\left(\beta^{\frac{3}{2}}\right)$ correction drops and we have

$$U(t) = \tilde{U}_0(t) \tilde{U}_1(t) + \mathcal{O}\left(\left(\beta^{\frac{3}{2}}\right)^{\frac{3}{2}} t_{max}\right). \quad (61)$$

After l -such iterations, we get the exact solution

$$U(t) = \tilde{U}_0(t) \tilde{U}_1(t) \cdots \tilde{U}_l(t) + \mathcal{O}\left(\beta^{\left(\frac{3}{2}\right)^l} t_{max}\right). \quad (62)$$

So the convergence of the scheme is super exponentially fast, close to the Newton type iteration.

We denote by t_{max} the maximum time we want to simulate our dynamics. The error in the MSA level l of the hierarchy denoted by ϵ can be written as

$$\epsilon = \beta^{\left(\frac{3}{2}\right)^l} t_{max}. \quad (63)$$

We can then invert this relation to obtain the number of desired hierarchy steps l for a given β and desired error ϵ ,

$$l > \frac{\log\left(\frac{\log \epsilon - \log t_{max}}{\log \beta}\right)}{\log\left(\frac{3}{2}\right)}. \quad (64)$$

in terms of $\tau_{max} = \beta t_{max}$ (see Eq. 8)

$$l > \frac{\log\left(\frac{\log \epsilon - \log \tau_{max}}{\log \beta} + 1\right)}{\log\left(\frac{3}{2}\right)} \quad (65)$$

5. Numerical implementation

The purpose of this section is to demonstrate that the multi-scale averaging method developed in [1] is superior to the standard split step method as it is much faster and the bound on the error can be estimated analytically. We will evolve the wave function for the model presented in Sec. 2 with the approximate evolution operator of the MSA method and compare the results to the ones found using the standard split step method. In the zeroth order we evolve the wave function with the help of (19), with U_0 calculated by (41).

The diagonalization (33) can also be performed once and can be done in parallel for the various time intervals. In particular the first order (23) requires to diagonalize $\bar{H}_1^{(j)}$ that in turn is given by the diagonalized $\bar{H}_0^{(j)}$ given by (16). This enables to compute the α_{k_1, k_0} of (39). To obtain the first order MSA approximate dynamics, we use the evolution operator

$$\hat{U}_1 = U_0 U_1, \quad (66)$$

where

$$\psi_1(x, t) = \hat{U}_1(t) \psi_1(x, 0) \quad (67)$$

where U_1 is given by (23) and $\bar{H}_1^{(j)}$ is given by (48). Taking into account the normal form transformation we use

$$U_{(\text{NF})} = \hat{U}_1 \tilde{U}^{-1}. \quad (68)$$

And in this order

$$\tilde{\psi}(x, t) = U_0 U_{(\text{NF})} \tilde{\psi}(x, 0)$$

This process is repeated l times and the error is estimated by (63).

The results are compared to the ones found with the help of the split step method. In this method the wave function is propagated keeping only the kinetic energy or the potential energy in small steps of size δt . The choice of a time step δt is crucial. The way to test the convergence of the scheme is by running the dynamics up to a point t using a time step δt , running the dynamics up to the same point t only using a new time step $\delta t' = \frac{1}{2}\delta t$. If the wave function is the same within some fixed accuracy then the scheme is assumed to be convergent. The accuracy is defined as

$$\delta_a(t) = \int_{\Gamma} dx |\psi_1^{(\delta t)}(x, t) - \psi_2^{(\frac{\delta t}{2})}(x, t)|^2. \quad (69)$$

Where Γ is the domain in space where the wave function is defined. If the error $\delta_a(t)$ is not small then one needs to continue adjusting until one converges. Listed in Table 1 are some values of the small parameter β and the time scale it dictates. For longer time scale a smaller and a more refined time step is needed in order to converge the split step method. For the values listed in Table 1 an accuracy of $\delta_a = 10^{-7}$ was chosen as a convergence criterion, i.e if the two wave functions obtained at the same time t with different time steps δt and $\frac{\delta t}{2}$ differed by less then $\delta_a = 10^{-7}$, the algorithm is considered converged and an appropriate choice of δt is obtained. The * marks the fact that the required time was too long for the standard split-step computation to converge.

To demonstrate the accuracy of the MSA method, we denote by $\psi_a(x, t)$ the wave function computed by the MSA method and by $\psi_s(x, t)$ the one found by the split step method and compute the deviation

$$\Delta(t) = \int_{\Gamma} dx |\psi_s(x, t) - \psi_a(x, t)|^2 \quad (70)$$

The initial wave function in all our computations is

$$\psi(x, t = 0) = \mathcal{N} e^{-\frac{x^2}{2(\sigma_x^0)^2}}, \quad (71)$$

where \mathcal{N} is the normalization constant. In Fig. 1 the comparison between the wave functions $\psi_s(x, t)$ and $\psi_a(x, t)$ is obtained by evolution starting from the initial wave function (71). It is presented for an arbitrary realization of the

random potential (11). The difference is very small and it will be calculated in what follows. The results are presented in Fig 2 where we plot

$$\bar{\Delta}(t) = \langle \Delta(t) \rangle_{\text{av}} . \quad (72)$$

The average is over 40 realizations of the potential $V(x, t)$ of (11). The averaging is performed as follows: $\Delta(t)$ is calculated for a specific realization and the average is taken so that the ϕ_i are distributed uniformly in the interval $[-\pi, \pi]$, while $v_n^{(r)}$ and k_n are distributed uniformly in the intervals $[v^{\min} = -15, v^{\max} = 15]$ and $[k^{\min} = -20, k^{\max} = 20]$ respectively (see Sec. 2 paragraph following Eq. 5). ω_n is calculated by (5). We take $\beta = 1 \cdot 10^{-3}$ and $\beta = 1 \cdot 10^{-4}$ while $\sigma_x^0 = 1$ resulting in the initial momentum standard deviation $\sigma_k^0 = 0.5$. In our basis Eqs. (33) and (34) for $|\varphi_j^k\rangle$, the largest value of the momentum is $|\tilde{k}| = 80$, therefore

$$|\tilde{k}| \gg \sigma_k^0 . \quad (73)$$

The largest value of $|x|$ is 10 therefore σ_x^0 is much smaller than the largest value of $|x|$, namely 10. To demonstrate the efficiency of the calculation we compare the computer time T_{comp} required to perform the numerical time propagation Fig. 2 up to times $t_{\max} = 8000$, we compare the results for the multi-scale and averaging split steps methods with the same precision $\delta_a = \epsilon = 10^{-7}$ we choose a time $t'_{\max} = T_0 \cdot \bar{i}$ such that \bar{i} is the smallest integer satisfying $t'_{\max} > t_{\max}$. the lowest hierarchy required for the calculation l is used. The results are summarized in table 2 and plotted in Fig 3. The calculations were performed on two computational nodes each composed of a 2.4 Ghz Intel Xeon processors.

β	v	T_0^2	T_0^4	δt for T_0^2	δt for T_0^4
$1 \cdot 10^{-2}$	100	100	10000	0.01	0.0009
$1 \cdot 10^{-3}$	1000	1000	1000000	0.01	0.0001
$5 \cdot 10^{-4}$	2500	2500	6250000	0.009	*
$1 \cdot 10^{-4}$	10000	10000	100000000	0.009	*

Table 1: split step time steps for different values of the small parameter. The accuracy is $\delta_a = 10^{-7}$

It turns out that for the problem we studied, the results we obtained are probably much better than the error estimate (63). To see this we present in table (3) the difference

$$\tilde{\Delta}_{l,l+1}(t) = \int_{\Gamma} dx |\psi_l(x, t_{max}) - \psi_{l+1}(x, t_{max})|^2 \quad (74)$$

as well as the bound (63) for $l = 3$ and $l = 4$ for different values of β and $t_{max} = T_0^2 = \frac{1}{\beta}$

β	$5 \cdot 10^{-5}$	$1 \cdot 10^{-4}$	$3 \cdot 10^{-3}$	$1 \cdot 10^{-2}$	$3 \cdot 10^{-2}$	$1 \cdot 10^{-1}$
T_0	141.42	100	18.25	10	5.77	3.162
\bar{i}	57	81	439	801	1386	2530
t'_{max}	8061.02	8100	8015	8010	8002.07	8000.56
l_{min}	3	3	4	5	5	6
T_{comp}^{av}	93	63	50	39	21	10
T_{comp}^{ss}	1220	960	740	124	60	30
$\frac{T_{comp}^{av}}{T_{comp}^{ss}}$	0.074	0.065	0.067	0.314	0.352	0.333

Table 2: The comparison between the computational time T_{comp}^{av} using the multi-scale averaging method and the computational time T_{comp}^{ss} using the split step method. Averaging over 40 realizations similar to the ones used in Fig. 2 was performed.

β	$5 \cdot 10^{-5}$	$1 \cdot 10^{-4}$	$3 \cdot 10^{-3}$	$1 \cdot 10^{-2}$	$3 \cdot 10^{-2}$	$1 \cdot 10^{-1}$
$\tilde{\Delta}_{3,4}$	$6 \cdot 10^{-11}$	$1.04 \cdot 10^{-10}$	$1.44 \cdot 10^{-10}$	$1.81 \cdot 10^{-10}$	$2.17 \cdot 10^{-12}$	$2.5 \cdot 10^{-10}$
$\epsilon_{l=3}$	$75 \cdot 10^{-8}$	$3.88 \cdot 10^{-7}$	$2.02 \cdot 10^{-6}$	$1.78 \cdot 10^{-5}$	$2.42 \cdot 10^{-4}$	$2.21 \cdot 10^{-3}$
$\epsilon_{l=4}$	$6.5 \cdot 10^{-10}$	$1.08 \cdot 10^{-9}$	$1.81 \cdot 10^{-9}$	$7.5 \cdot 10^{-8}$	$6.5 \cdot 10^{-7}$	$8.66 \cdot 10^{-5}$

Table 3: The difference (74) and the bound (61) for various values of β and $t_{max} = T_0^2 = \frac{1}{\beta}$.

6. Spreading in k-space

MSA enables us to calculate very accurately the spreading in momentum space over a very long time. For this purpose we evolve the wave function $\psi(x, t)$ starting from (71) with $\sigma_x^0 = 1$ for the potential (11). The wave function is used to calculate the variance of the momentum

$$\text{Var}_k(t) = \int \hat{\psi}^*(k, t) (k - \bar{k})^2 \hat{\psi}(k, t) dx \quad (75)$$

where

$$\bar{k} = \int \hat{\psi}^*(k, t) k \hat{\psi}(k, t) dx \quad (76)$$

and $\hat{\psi}(k, t)$ is the Fourier transform of $\psi(x, t)$. Then we calculate the spread of the momentum relative to initial one

$$\Delta \text{Var}_k^{(n)}(t) = \frac{\text{Var}_k(t) - \text{Var}_k(0)}{\text{Var}_k(0)}. \quad (77)$$

This calculation is performed for each realization of the random potential. Then average over 40 realizations of the random potential was performed as in (72), namely we calculate

$$\bar{\Delta}_v(\tau) = \left\langle \Delta \text{Var}_k^{(n)}(t) \right\rangle_{\text{av}} \quad (78)$$

It is plotted as a function of $\tau = \beta t$ in Fig. 4. Because of the smallness we conclude that the replacement of the Hamiltonian by a finite matrix does not effect the result (see Eq. (73)). The plot is smoothed by averaging over intervals of length $\Delta\tau = 10^2$, leading to the results presented in Fig. 5. The calculation

is repeated for several values of β , and in Fig. 6 the results are fitted to the formula

$$\bar{\Delta}_v(\tau) = C(\beta) \tau^{\alpha(\beta)}. \quad (79)$$

From the plot it is reasonable to extrapolate

$$\lim_{\beta \rightarrow 0} C = \lim_{\beta \rightarrow 0} \alpha = 0. \quad (80)$$

We conclude that in the limit $\beta \rightarrow 0$ the spreading stops. This is the limit where the velocity is much larger than the Chirikov resonant velocities $v_n^{(r)}$ of Eq. (5). This leads us to the conjecture that if in one dimension the $v_n^{(r)}$ are bounded, the kinetic energy cannot grow to infinity, in spite of the driving.

In Fig. 7, the classical and quantum results are compared. The quantum results were computed as the ones for Fig. 4 while for the classical results 60 initial conditions were also chosen at random from a Gaussian distribution corresponding to the initial quantum wave function $\psi(x, 0)$ of (71). Both classical and quantum results were averaged over 40 realizations of the random potential. We note that both classical and quantum spreading in momentum stop. The classical spreading stops at an earlier stage.

acknowledgments

This work was partly supported by the Israel Science Foundation (ISF), grant 1028/12, by the US-Israel Binational Science Foundation (BSF), grant 2010132, by the USA National Science Foundation (NSF DMS 1201394) and by the Shlomo Kaplansky academic chair. T.K. thanks the MIT physics of living systems institute where part of this work was done. Part of this work was done while T.K. and A.S. visited CCNU, China. T.K. acknowledges the grateful support of David Cohen and the ATLAS-Technion grid project for computational resources. We would like to thank the referee for critical reading and insightful comments of the first version of the manuscript.

7. Appendix

The numerical methodology presented and the results obtain relies on the rigorous frame presented by Fishman and Soffer [1]. In order to clarify the methodology we present here a concise summary and explanation of the rigorous foundations for our numerical MSA method. We consider the following equation of motion

$$i \frac{\partial}{\partial t} \vec{\psi} = \beta H(t) \vec{\psi} \quad (81)$$

where β is a small parameter, $\vec{\psi}$ is a finite vector quantity and $H(t)$ is a hermitian matrix. The multiscale method used in [1] and subsequently in this paper is based on partial time averaging of the propagator, repeated on larger and larger scales. The averaging on a cascade of larger and larger scales results in a hierarchy of averaged dynamical equations. This in turn will let us, in contrast to known time averaging analysis [24, 25], to extend the time averaging to arbitrary time intervals. We start by constructing an average of $H(t)$ over an interval of length T_0

$$\bar{H}_0^{(n)} = \frac{1}{T_0} \int_{nT_0}^{(n+1)T_0} H(t) dt \quad \text{for} \quad nT_0 \leq t < T_0(n+1). \quad (82)$$

where the relation between T_0 and β is $T_0 = \frac{1}{\sqrt{\beta}}$. The above defines an averaged dynamical process, this can be written in the form of a propagator which generates partially averaged motion.

$$U_0(t) = e^{-i\beta \bar{H}_0^{(n)}(t-nT_0)} \dots e^{-i\beta \bar{H}_0^{(0)}T_0} \quad \text{for} \quad nT_0 \leq t \leq (n+1)T_0, \quad (83)$$

and its inverse

$$U_0^{-1}(t) = e^{+i\beta \bar{H}_0^{(0)}T_0} e^{+i\beta \bar{H}_0^{(1)}T_0} \dots e^{i\beta \bar{H}_0^{(n)}(t-nT_0)}. \quad \text{for} \quad nT_0 \leq t \leq (n+1)T_0. \quad (84)$$

Both the propagator and its inverse admit an equation of motion of the form

$$i \frac{\partial}{\partial t} U_0(t) = \beta \bar{H}_0^{(n)} U_0(t) \quad \text{for} \quad nT_0 \leq t \leq (n+1)T_0$$

$$i \frac{\partial}{\partial t} U_0^{-1}(t) = U_0^{-1} \left(-\beta \bar{H}_0^{(n)} \right) = -\beta U_0^{-1} \bar{H}_0^{(n)}(t) \quad \text{for} \quad nT_0 \leq t \leq (n+1)T_0.$$

As shown in Lemma 1 of [1], the above generated partially averaged dynamics differ from the full dynamics by.

$$\left\| \int_0^t (H(t') - \bar{H}_0(t')) dt' \right\| \leq 2 \|H\|_t T_0.$$

The above given bound is used for the first stage of the averaging hierarchy. To show this let us construct the rest of the averaged hierarchy; we start by writing the solution of the averaged equation

$$\vec{\psi}_1(t) = U_0^{-1}(t) \vec{\psi}(t), \quad (85)$$

the solution admits an equation of motion

$$\begin{aligned} i \frac{\partial}{\partial t} \vec{\psi}_1 &= \left[i \frac{\partial}{\partial t} U_0^{-1}(t) \right] \psi(t) + U_0^{-1}(t) \left[i \frac{\partial}{\partial t} \vec{\psi}(t) \right] \\ &= \left[-\beta U_0^{-1} \bar{H}_0^{(n)}(t) \right] \psi(t) + U_0^{-1} [\beta H(t) \vec{c}(t)], \end{aligned} \quad (86)$$

we rewrite Eq. (86) using Eq. (85)

$$\begin{aligned} i \frac{\partial}{\partial t} \vec{\psi}_1(t) &= -\beta U_0^{-1} \bar{H}_0^{(n)}(t) U_0(t) \vec{\psi}_1(t) + \beta U_0^{-1} H(t) U_0(t) \vec{\psi}_1(t) \\ &= \beta U_0^{-1} \left[H(t) - \bar{H}_0^{(n)}(t) \right] U_0(t) \vec{\psi}_1(t). \end{aligned} \quad (87)$$

By denoting

$$H_1(t) = U_0^{-1} \left[H(t) - \bar{H}_0^{(n)}(t) \right] U_0(t)$$

Eq (87) can be written analogous to (81)

$$i \frac{\partial}{\partial t} \vec{\psi}_1(t) = \beta H_1(t) \vec{\psi}_1(t)$$

and in the same way as (82) we can define

$$\bar{H}_1^{(n)} = \frac{1}{T_0} \int_{nT_0}^{(n+1)T_0} H_1(t) dt \quad \text{for} \quad nT_0 \leq t < T_0(n+1).$$

\bar{H}_1 has an associated propagator analogous to (83) and (84)

$$\begin{aligned} U_1(t) &= e^{-i\beta \bar{H}_1^{(n)}(t-nT_0)} \dots e^{-i\beta \bar{H}_1^{(0)}T_0} \\ U_1^{-1}(t) &= e^{i\beta \bar{H}_1^{(0)}T_0} \dots e^{i\beta \bar{H}_1^{(n)}(t-nT_0)}. \end{aligned}$$

Furthermore

$$\|\bar{H}_1\| \leq c\sqrt{\beta}$$

(see the proof of Thm 1 of [1])

From this we arrive at the following approximation:

$$\psi(t) = U_0(t) \psi_1(t)$$

and for all $T_i < t < T_f$

$$\sup_{T_i \leq t \leq T_f} \|\psi_1(t) - \psi_1(T_i)\| \leq c \left(\sqrt{\beta} + \beta^{3/2} |T_f - T_i| + \beta^{5/2} |T_f - T_i|^2 \right).$$

Normal Forms

Inspection of the proof shows that the error term $\sqrt{\beta}$ comes from the boundary terms, after integration by parts. This boundary term can be absorbed by a change of variables and the new variables $\tilde{\psi}_1$ is better behaved. This way of introducing normal form transformations, via integration by parts and

$$\psi_1 \rightarrow \tilde{\psi}_1$$

originally developed in [26] and adapted to averaging in ref [1].

$$\tilde{\psi} \equiv \tilde{U} \psi_1 \equiv \left(I + i\beta \int_{T_i}^t H_1(s) ds \right) \psi_1(t)$$

where I stands for the identity operator. Then, we have that(Thm 2 of [1])

$$\psi(t) = U_0 \tilde{U}^{-1} \tilde{\psi}_1(t) = U_0(t) \psi_1(t)$$

and

$$\sup_{T_i \leq t \leq T_f} \left\| \tilde{\psi}_1(t) - \tilde{\psi}_1(T_i) \right\| \leq C \left(|T_f - T_i| + \beta |T_f - T_i|^2 \right) \beta^{3/2}.$$

We now write the next step of the iteration:

$$i \frac{\partial}{\partial t} U_1(t) = \beta \bar{H}_1(t) U_1(t) = \beta^{3/2} \left(\frac{\bar{H}_1}{\sqrt{\beta}} \right) U_1(t) \quad (88)$$

and similarly for U_1^{-1} .

Now defining the partial solution

$$\psi_2(t) = U_1^{-1}(t)\psi_1(t) \quad (89)$$

and develop an equation of motion :

$$\begin{aligned} i\frac{\partial}{\partial t}\psi_2(t) &= \left[i\frac{\partial}{\partial t}U_1^{-1}(t) \right] \psi_1(t) + U_1^{-1}(t) \left[i\frac{\partial}{\partial t}\psi_1(t) \right] = \\ &- \beta U_1^{-1}\bar{H}_1(t)U_1\psi_2(t) + \beta U_1^{-1}\bar{H}_1(t)U_1(t)\psi_2(t) \end{aligned} \quad (90)$$

reducing to

$$i\frac{\partial}{\partial t}\psi_2(t) = \beta U_1^{-1}(t) [H_1(t) - \bar{H}_1(t)] U_1(t)\psi_2(t). \quad (91)$$

Define

$$H_2(t) = U_1^{-1} [H_1(t) - \bar{H}_1(t)] U_1(t), \quad (92)$$

leading to

$$i\frac{\partial}{\partial t}\psi_2 = \beta H_2(t)\psi_2(t). \quad (93)$$

In fact, the above step in the hierarchy can be evaluated in the same manner and as was shown in [1] this is bounded

$$\left\| \int_0^t (H(t') - \bar{H}_1(t')) dt' \right\| \leq \left(\frac{c}{\sqrt{\beta}} \right) + c\beta t$$

Combining this iterate with a normal form transformation we obtain (Thm 3 of Ref [1])

$$\psi(t) = U_0(t)U_1(t)\tilde{U}_2^{-1}\psi_2(t)$$

where \tilde{U}_2 is the appropriate normal form transformation, and,

$$i\partial_t\psi_2(t) = \beta^{3/2}\tilde{H}(t)\psi_2(t)$$

and $\tilde{H}(t)$ satisfies the same conditions and bounds as the original Hamiltonian.

Therefore the error bound we have is now given by the error bound on the equations with

$$\beta \rightarrow \beta^{3/2}.$$

So, after n such iterations, the error bound is of order $\beta^{(3/2)^n}$.

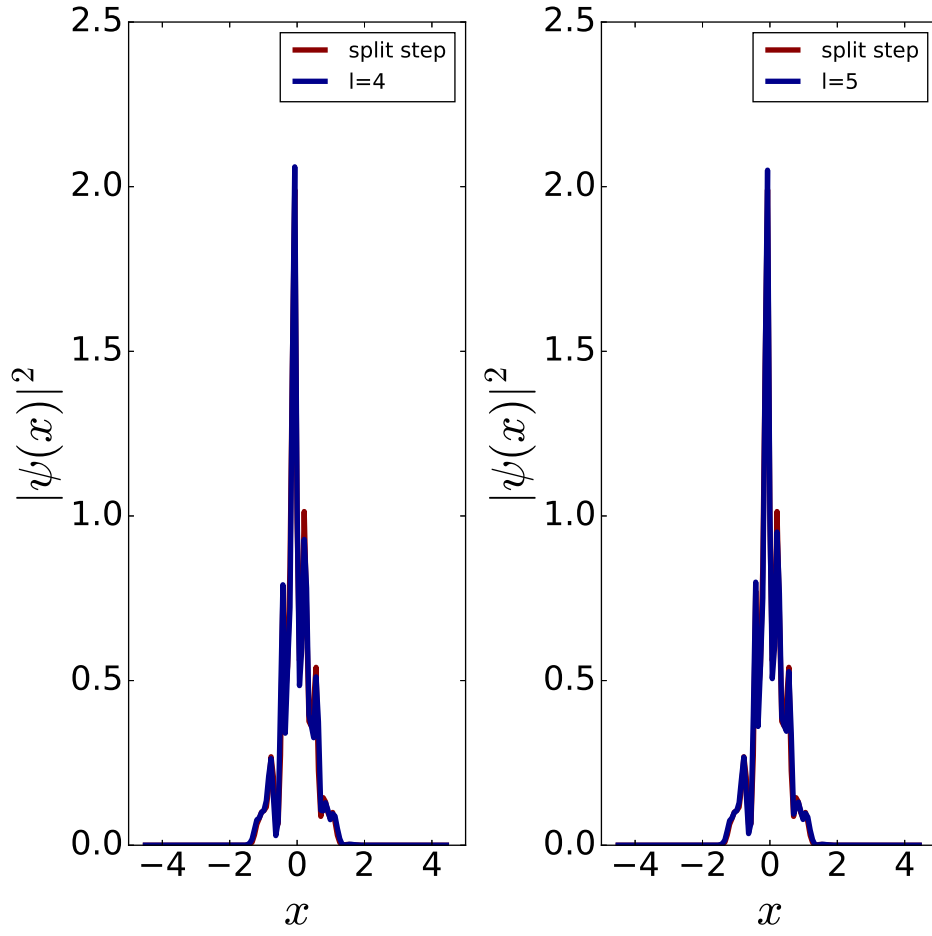


Figure 1: The wave function at time $t = T_0 = \frac{1}{\sqrt{\beta}}$ obtained from the averaging method with precision of $\epsilon = 10^{-7}$ and the split step method with accuracy of $\delta_a = 10^{-7}$ for $\beta = 10^{-3}$ and $\sigma_x^0 = 1.0$. Two cases of multi-scale and averaging are presented (a) The fourth level of the hierarchy ($l = 4$, Eq. 63) (b) The fifth level of the hierarchy ($l = 5$, Eq. 63).

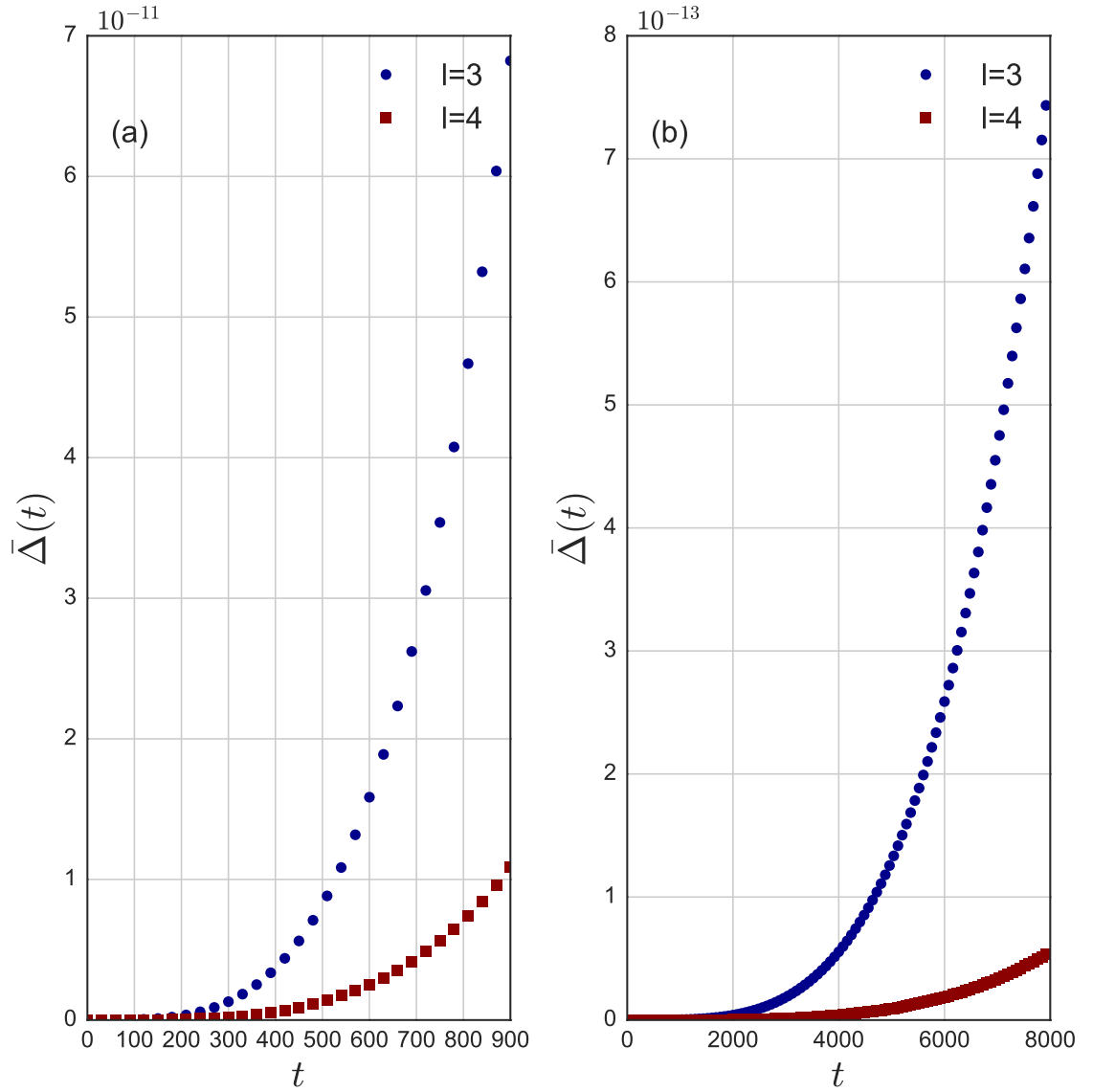


Figure 2: The average difference $\bar{\Delta}(t)$ (Eqs. 72,67) between the split step and averaging method as calculated for two different values of (a) $\beta = 10^{-3}$ and (b) $\beta = 10^{-4}$ while $\sigma_x^0 = 1.0$. Each subfigure presents both calculations for the third and fourth level in the hierarchy ($l = 3, 4$ Eq. 63) . The precision required is $\epsilon = \delta_a = 10^{-7}$

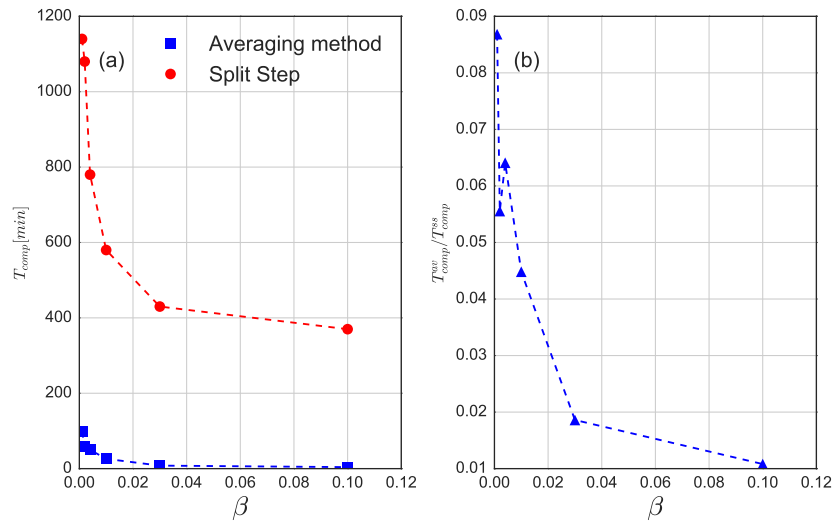


Figure 3: Computational benchmark (run time) as a function of β as presented in Table 2. (a) Run times, obtained for split step method (T_{comp}^{ss}) and for the multiple scale and averaging (T_{comp}^{av}) method. The precision required was $\epsilon = \delta_a = 10^{-7}$ and the values of l are presented in table 2. (b) The ratio $\frac{T_{comp}^{av}}{T_{comp}^{ss}}$ presented in table 2.

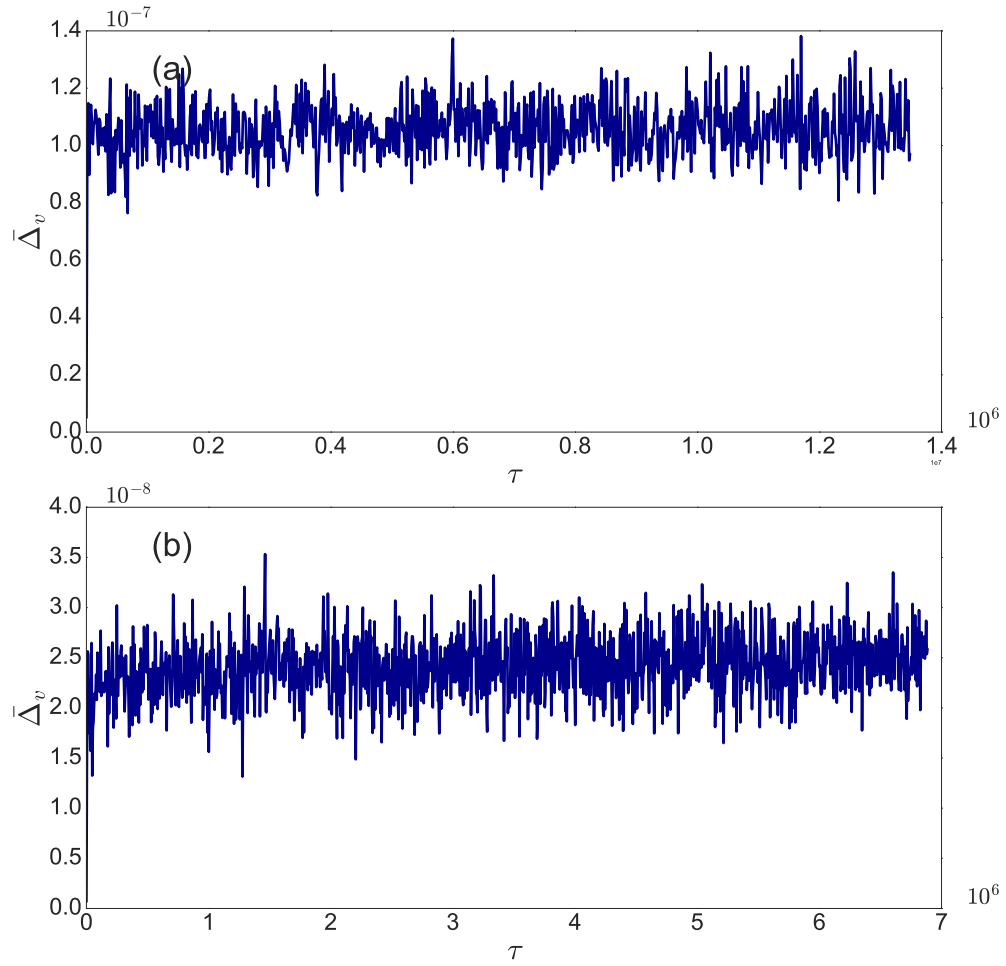


Figure 4: The average spread of the kinetic energy $\bar{\Delta}_v$ of Eq. (78) of a quantum wave function obtained for the multi-scale and averaging method with (a) $\beta = 5 \cdot 10^{-3}$ and $l = 9$ (b) $\beta = 1 \cdot 10^{-4}$ and $l = 8$. For both cases $\epsilon = 10^{-10}$. Note that the hierarchy used here is much higher than required for the precision ϵ .

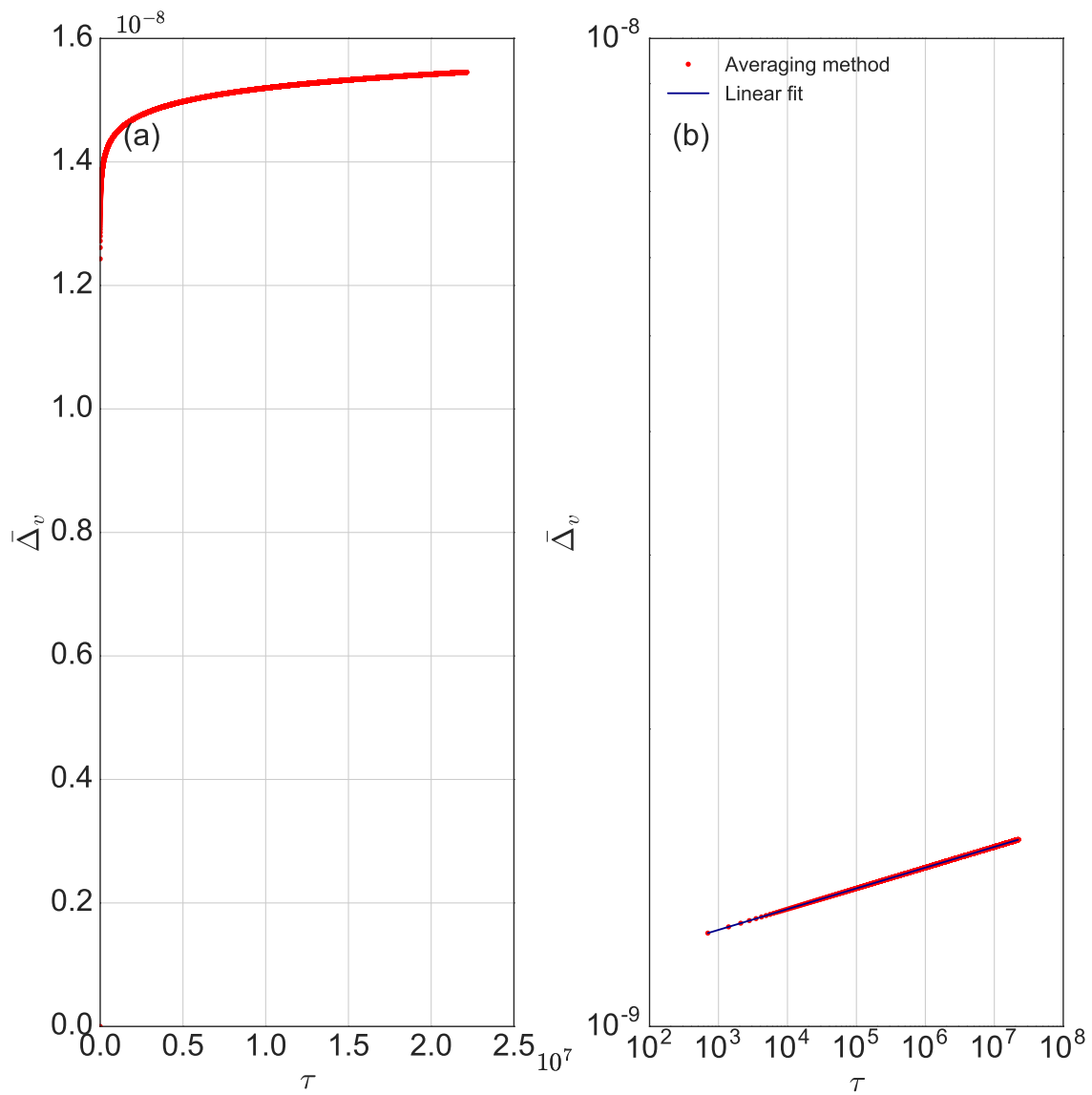


Figure 5: $\bar{\Delta}_v(\tau)$ smoothed over time intervals $\Delta\tau = 10^2$ as a function of τ on (a) regular scale (b) logarithmic scale, for $\beta = 10^{-4}$, $\epsilon = 10^{-10}$ and $l = 6$.

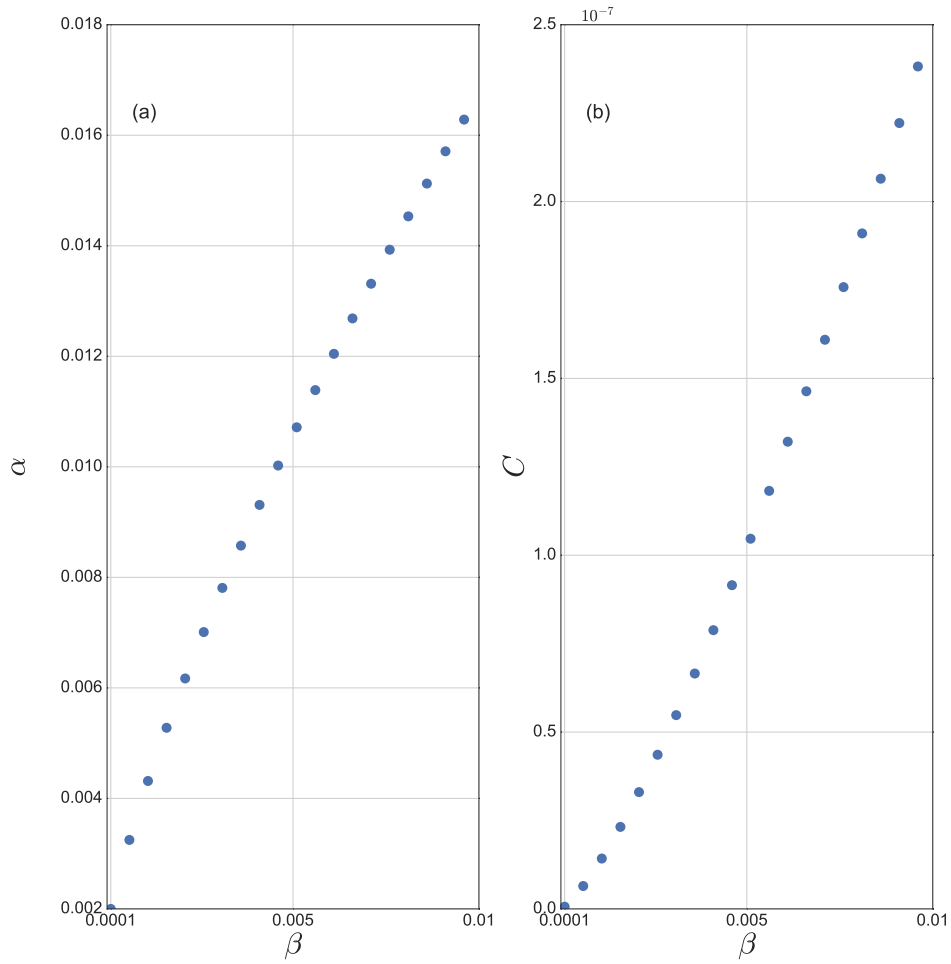


Figure 6: The parameters of the fit (79) as a function of β

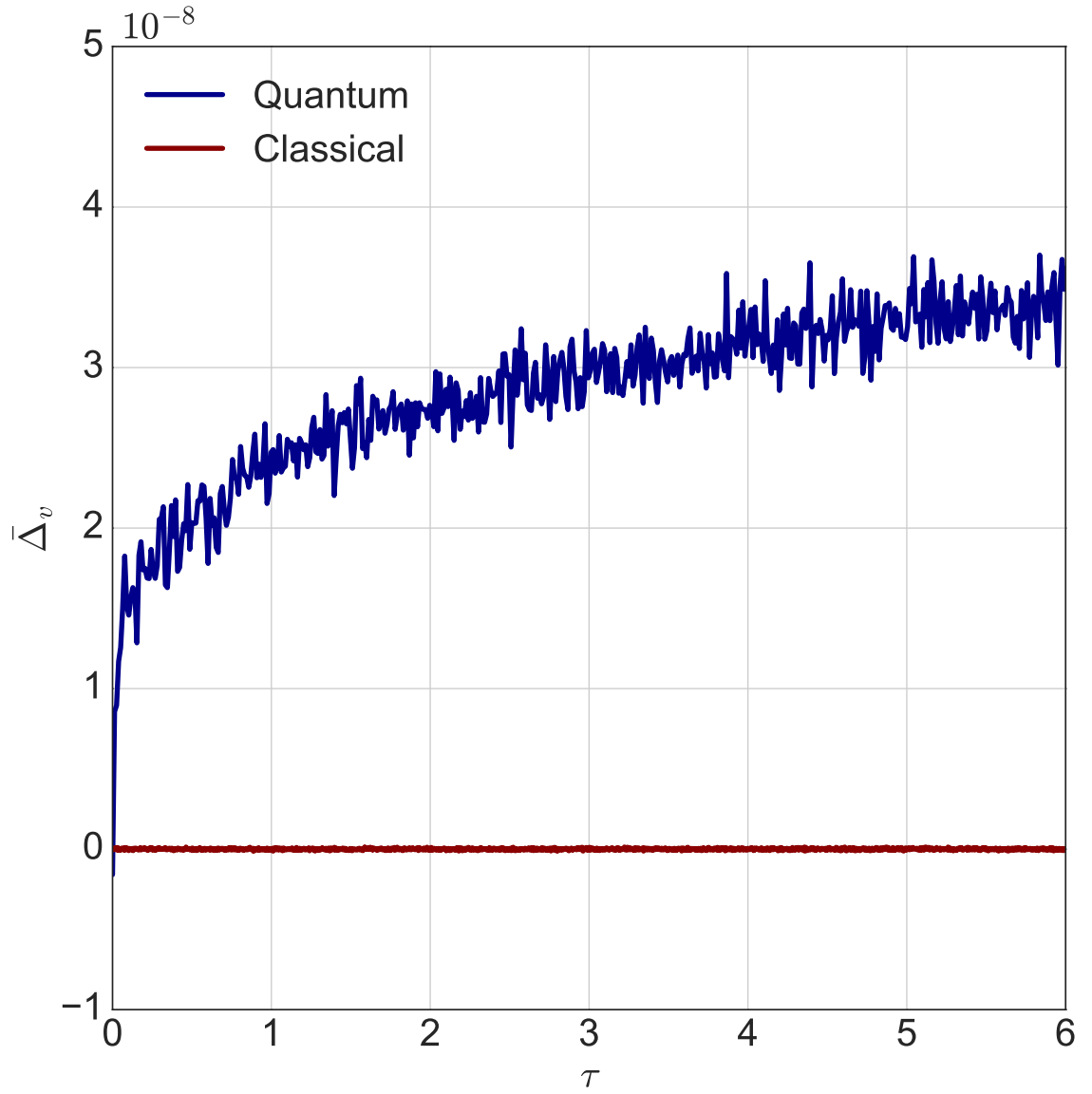


Figure 7: The average spreading of the quantum and classical kinetic energy. The quantum results were found with the multi-scale and averaging method and the classical result is obtained via standard Runge Kutta integration with integration threshold of 10^{-10} . The parameters used are the same as in Fig. 4, but $l = 6$

References

References

- [1] S. Fishman, A. Soffer, Multiscale time averaging, reloaded, *SIAM Journal on Mathematical Analysis* 46 (2) (2014) 1385–1405.
- [2] L. Levi, Y. Krivolapov, S. Fishman, M. Segev, Hyper-transport of light and stochastic acceleration by evolving disorder, *Nature Physics* 8 (12) (2012) 912–917.
- [3] Y. Krivolapov, L. Levi, S. Fishman, M. Segev, M. Wilkinson, Super-diffusion in optical realizations of anderson localization, *New Journal of Physics* 14 (4) (2012) 043047.
- [4] Y. Krivolapov, S. Fishman, Universality classes of transport in time-dependent random potentials, *Physical Review E* 86 (3) (2012) 030103.
- [5] Y. Krivolapov, S. Fishman, Transport in time-dependent random potentials, *Physical Review E* 86 (5) (2012) 051115.
- [6] Y. Maday, A. T. Patera, E. M. Rønquist, An operator-integration-factor splitting method for time-dependent problems: application to incompressible fluid flow, *Journal of Scientific Computing* 5 (4) (1990) 263–292.
- [7] R. Kosloff, Time-dependent quantum-mechanical methods for molecular dynamics, *The Journal of Physical Chemistry* 92 (8) (1988) 2087–2100.
- [8] G. Uhlenbeck, L. Ornstein, On the theory of the brownian motion, *Physical Review letters* 36 (1930) 823–841.
- [9] P. Sturrock, Stochastic acceleration, *Physical Review letters* 141 (1966) 186–191.
- [10] C. Gardiner, *Stochastic methods*, Springer-Verlag, Berlin–Heidelberg–New York–Tokyo, 1985.

- [11] V. Bezuglyy, B. Mehlig, M. Wilkinson, K. Nakamura, E. Arvedson, Generalized ornstein-uhlenbeck processes, *Journal of Mathematical Physics* 47 (7).
- [12] E. Arvedson, M. Wilkinson, B. Mehlig, K. Nakamura, Staggered ladder spectra, *Physical Review letters* 96 (2006) 030601.
- [13] M. N. Rosenbluth, Comment on “classical and quantum superdiffusion in a time-dependent random potential”, *Physical Review letters* 69 (1992) 1831–1831.
- [14] L. Golubović, S. Feng, F.-A. Zeng, Classical and quantum superdiffusion in a time-dependent random potential, *Physical Review letters* 67 (1991) 2115–2118.
- [15] J. S. Hesthaven, S. Gottlieb, D. Gottlieb, *Spectral methods for time-dependent problems*, Vol. 21, Cambridge University Press, 2007.
- [16] C. Leforestier, R. Bisseling, C. Cerjan, M. Feit, R. Friesner, A. Guldborg, A. Hammerich, G. Jolicard, W. Karrlein, H.-D. Meyer, et al., A comparison of different propagation schemes for the time dependent schrodinger equation, *Journal of Computational Physics* 94 (1) (1991) 59–80.
- [17] U. M. Ascher, S. J. Ruuth, B. T. Wetton, Implicit-explicit methods for time-dependent partial differential equations, *SIAM Journal on Numerical Analysis* 32 (3) (1995) 797–823.
- [18] T. Schwartz, G. Bartal, S. Fishman, M. Segev, Transport and anderson localization in disordered two-dimensional photonic lattices, *Nature* 446 (7131) (2007) 52–55.
- [19] M. Piraud, P. Lugan, P. Bouyer, A. Aspect, L. Sanchez-Palencia, Localization of a matter wave packet in a disordered potential, *Physical Review A* 83 (3) (2011) 031603.

- [20] J. Billy, V. Josse, Z. Zuo, A. Bernard, B. Hambrecht, P. Lugan, D. Clement, L. Sanchez-Palencia, P. Bouyer, A. Aspect, Direct observation of anderson localization of matter waves in a controlled disorder, *Nature* 453 (7197) (2008) 891–894.
- [21] L. Sanchez-Palencia, D. Clement, P. Lugan, P. Bouyer, G. V. Shlyapnikov, A. Aspect, Anderson localization of expanding bose-einstein condensates in random potentials, *Physical Review Letters* 98 (21) (2007) 210401.
- [22] B. V. Chirikov, A universal instability of many-dimensional oscillator systems, *Physics Reports* 52 (5) (1979) 263 – 379.
- [23] G.M.Zaslavski., B. Chirikov, Stochastic instability of non-linear oscillations, *Soviet Physics Uspekhi* 14 (5) (1972) 549.
- [24] J. A. Sanders, F. Verhulst, J. Murdock, *Averaging Methods in Nonlinear Dynamical Systems*, 2nd Edition, Springer, 2010.
- [25] M. S. Krol, On the averaging method in nearly time-periodic advection-diffusion problems, *SIAM J. Appl. Math.* 51 (1991) 1622–1637.
- [26] A. Soffer, M. I. Weinstein, Resonances, radiation damping and instability in hamiltonian nonlinear wave equations, *Inventiones mathematicae* 136 (1) (1999) 9–74.